Nuclear pores and membrane holes: generic models for confined chains and entropic barriers in pore stabilization†

Peter J. Photos, Harry Bermudez, Helim Aranda-Espinoza, Julian Shillcock and Dennis E. Discher

Received 7th August 2006, Accepted 4th October 2006
First published as an Advance Article on the web 27th October 2006
DOI: 10.1039/b611412c

The lumen of the nuclear pore complex is increasingly understood to be lined by a polymer brush that entropically regulates transport in and out of the nucleus—and it seems likely that similar effects probably arise with glycocalyx-lined holes in cell membranes. Here we mimic such pore-confined brushes with self-assembled polymer membranes imbued with nano-holes. Experiment and theory help elucidate the entropic origin and stabilization of the pores, which appear to have a similar basis as steric stabilization of colloids bearing polymer brushes. Free energies of interacting brushes reveal stable minima at pore sizes *smaller* than the classical metastable point, with little effect of the particular pore geometry. Such entropic forces have potential implications for lock and key mechanisms of nuclear pore assembly as well as transient poration of cells and synthetic nano-pores with regulatory mechanisms for transport.

1. Introduction

Rapid fluctuations of large, natively unfolded nucleoporin proteins (Fig. 1) reportedly form an entropic barrier to would-be entrants into the nuclear pore complex.[1] Recent measurements of the forces exerted by clusters of nucleoporin chains indeed demonstrate a large excluded volume typical of polymer brushes that lack attractive interactions. Dedicated transport proteins are believed to enter or leave the cell nucleus by binding the brush and decreasing its entropy. Such brushes are likewise expected to exert forces on the walls of the nuclear pore complex, which motivates the experimental and theoretical models here.

For several decades, insight into membrane pores has been obtained from considerable work on lipid vesicles, but the small headgroups of lipids are unlikely to contribute much in the way of entropy-dominated interactions that are typical of brushes within nuclear pores or related structures. With purely synthetic amphiphiles composed in part of brushy hydrophilic chains,[2–4] physical properties such as brush thickness can be easily varied and processes such as poration can be both simulated and imaged (Fig. 1). Using a modified version of electroporation[5] we have recently reported seemingly unique, stable membrane pores[6,7] that inspire comparisons to the nuclear pore complex. Pore dynamics prove to be strongly dependent on the hydrophobic core thickness d, which scales with polymer molecular weight M_n:[3] indeed, membrane response in poration differs greatly for small *versus* large d. Here, we theorize on the basis for the post-poration divergence seen with vesicles formed from diblocks either of poly(ethylene oxide)–polybutadiene (PEG–PBD, denoted 'OB') or of a related hydrogenated ('OE') diblock (Table 1). After electroporation, all vesicles form visible pores immediately after poration (Fig. 2A). Vesicles consisting of thinner membranes either reseal completely, or, like OB16, rupture from their initial pore (Fig. 2A, *top*).[6] Similar dynamics in lipid vesicles have been reported, for example, by the Brochard-Wyart group using glycerol to slow down pore growth.[8,9] In contrast,

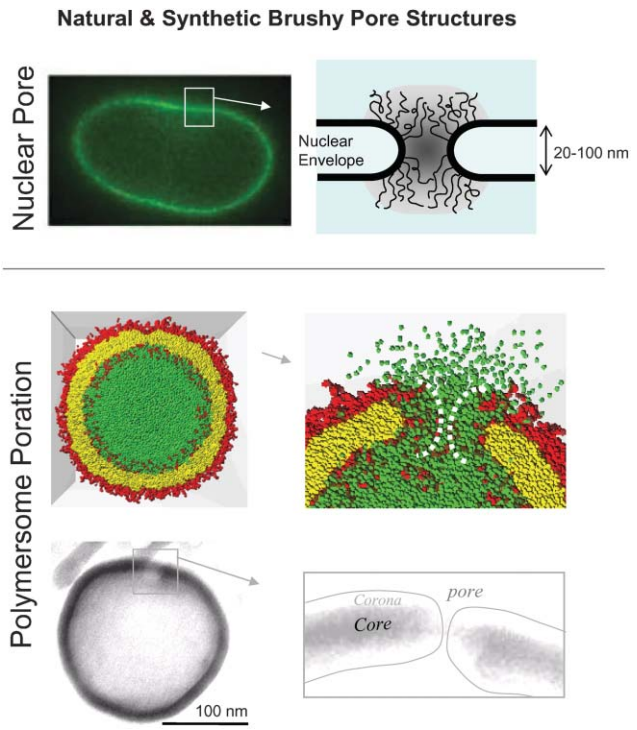

Fig. 1 Natural and synthetic brushy pore structures. The nuclear pore complex regulates transport into and out of the nucleus. Simulations of block copolymer vesicles with pores are done by dissipative particle dynamics,[4] and the cryo-TEM of porated vesicles is done on biodegradable polymersomes.[10]

Laboratory for Research on the Structure of Matter, University of Pennsylvania, Philadelphia, Pennsylvania 19104
E-mail: discher@seas.upenn.edu; Fax: +1 (215) 573-2093;
Tel: +1 (215) 898-4809
† This paper is part of a *Soft Matter* themed issue on Proteins and Cells at Functional Interfaces. Guest editor: Joachim Spatz.

Table 1 Vesicle types discussed in this paper and their properties. The brush length, L_0, is determined by the Alexander–de Gennes scaling relation, $L_0 = Na^{5/3}\sigma_0^{1/3}$, and the "grafting" density, σ_0, is determined by the scaling $\sigma_0 \sim N^{-0.3}$, and σ_0 for OE7 experimentally determined to be 0.159 molecule nm^{-2}.[1] The core thickness, d, as well as the lytic tension, τ_{lysis}, is obtained from ref. 3

Vesicle type	Amphiphile	M_n/Da	D_0/nm	PEG length/nm	d_{core}nm[a]	τ_{lysis}mN nm
SOPC	C_{18}phospholipid	790	—	—	3.0	9.0
OB_2	EO_{28}–BD_{48}	3600	1.2	4.0	9.6	14
OE7	EO_{40}–EE_{37}	3900	1.3	5.3	8.0	20
OB16	EO_{50}–BD_{55}	5200	1.3	6.8	10.6	19
OB18	EO_{80}–BD_{125}	10 400	1.6	11.0	14.8	33
OB19	EO_{150}–BD_{250}	20 000	1.8	19.8	21	22

[a] ± 1 nm.

polymer vesicles with thick membranes like OB18 and OB19 do not rend: the vesicles retain their shape but lose phase contrast long after the initial pore disappears (Fig. 1A, *bottom*). This loss of contrast—a direct result of encapsulant loss—is presumably due to semipermanent pore formation.

The lifetime of such pore formation is of broad interest: a permanent or long-lasting pore may result in a vesicle with unique release kinetics, especially for drug delivery[10,11] and DNA permeation.[11–13] A gated pore that more closely mimics the regulated macromolecular transport of the nuclear pore complex could also be a useful nano-filter. However, the extended lifetime of pores in polymer membranes might not be thermodynamic—their existence could be metastable and long-delayed in resealing, *i.e.* kinetically trapped. Long lasting pores can also be achieved through direct physical manipulation of the membrane. Zhelev and Needham,[14] for example, have reported pores in lipid vesicles that last for seconds under sustained tension after electroporation. We hypothesize here that the pores in polymersome membranes are indeed thermodynamically stable after initial formation. We base this premise on previous observations of long-lasting pores, without external manipulation, of seemingly inveterate sizes and a distinctive dependence on membrane thickness but no strong dependence on vesicle size, at least for giant vesicles of 5–20 μm radius. Previous work also shows that smaller molecules escape with simple kinetics, while larger, fluorescently labeled dextrans do not, even at long times, which suggests a limited yet constant pore size.[6] Additionally, long after poration and loss of phase contrast, vesicles fail to retain their integrity upon aspiration by a micropipette. As shown in Fig. 2A, vesicles are unable to sustain even a modest tension, and instead collapse completely. Such behavior was observed up to tens of minutes after poration and subsequent content leakage. On the same time scales, thinner membranes that initially show "classical" behavior of vesicle rupture can actually reform vesicles,[6] a direct result of the strong energetic preference of a closed vesicle structure.

With our current repertoire of block copolymers, only the two largest copolymers—OB18 and OB19—form vesicles that yield these apparently stable pores. The contrasting behavior to that of thinner membranes—*e.g.* those of OE7 and OB2—suggests that polymer length plays a key role. Specifically, the

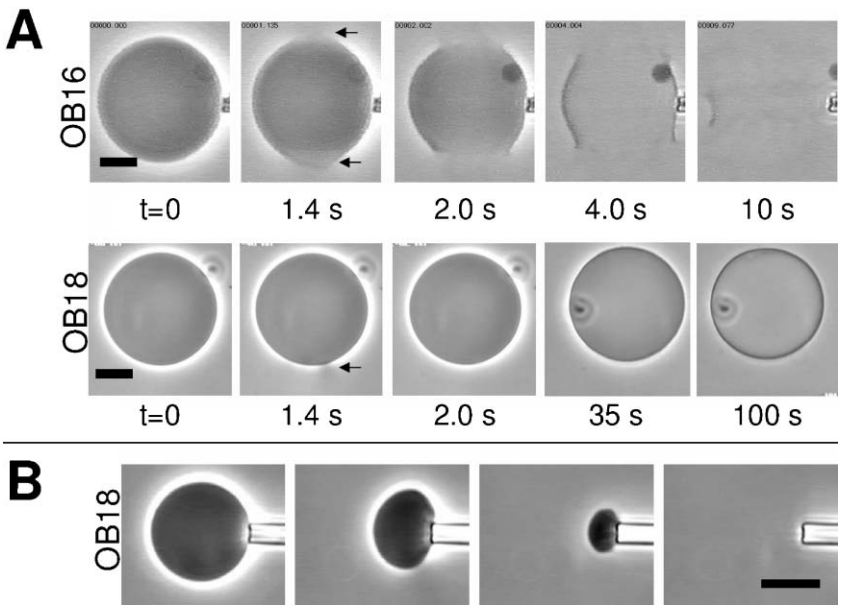

Fig. 2 (**A**) Polymersome behavior following electroporation. Both OB16 (*top*) and OB18 (*bottom*) show initial pore formation within seconds after voltage discharge. The pore in OB16 continues to grow until total vesicle rending, obeying eqn (1). OB18 vesicles, by contrast, no longer have any large visible pores after two seconds, suggesting resealing. However, over long periods of time, loss of phase contrast is observed, corresponding to content leakage. (**B**) Sequential frames of micropipette aspiration of OB18 after poration. The vesicle rapidly collapses despite an apparently intact membrane, suggesting long-lived nano-sized pores. Such behavior is seen even tens of minutes after poration. Scale bars are 20 μm.

thicker hydrophobic membrane and the longer PEG corona could effect a stabilization of the pores formed during electroporation. The suggestion of PEG stabilization of morphology is not new; PEG has long been known to limit aggregation between colloidal particles.[15–17] Here, however, we hypothesize that the PEG stabilizes an *inner* substructure. It should be noted that although it is conceivable that PEG chains may simply kinetically trap resealing pores, entanglements of chains are only dominant in the larger of the two polymers (OB19).[3]

2. Modeling sterically stabilized pores

The behavior of our thicker membranes sharply contrasts with that observed in typical lipid membranes, where pores are observed to either reseal quickly or completely rend the membrane, with only a few notable exceptions.[8,14] A simple, classical energy balance matches the behavior of such lipid-based pores remarkably well. First described by Derjaguin *et al.*,[18] the surface and edge energies balance for a pore of size R in an infinitely thin membrane:

$$E_{\text{pore}} = 2\pi R\Gamma - \pi R^2\Sigma \quad (1)$$

Here Γ is the edge energy per length (line tension) and Σ is the surface energy per area (interfacial tension). At a critical pore size $R^* = \Gamma/\Sigma$, an unstable pore is predicted, such that pores smaller than R^* reseal and those larger than R^* grow until membrane disintegration. This result has been observed repeatedly.[14,19,20]

Our observations of long-lived, and at least metastable pores in giant vesicles, suggests that our polymeric systems impart an additional contribution to the overall energy. We hypothesize that the PEG segments lining the pores create a steric barrier to resealing, possibly keeping pores open indefinitely (Fig. 3A). These "hairy" holes are thus stabilized in a manner very similar to that of colloids by grafted polymers, albeit with very different geometries.[15] The free energy contribution from the PEG brush ΔG_{brush} is thus a new term added to the traditional pore energy,

$$E_{\text{pore}} = 2\pi R\Gamma - \pi R^2\Sigma - \Delta G_{\text{brush}} \quad (2)$$

In eqn (1) and (2), the interfacial tension, Σ, is an empirical parameter that represents the interactions between the hydrophobic (poly(butadiene)) and hydrophilic (poly(ethyleneoxide)) blocks. Since we are applying an electric field to produce the pore in the membrane, the pore formation occurs through membrane stretching,[7] and we therefore assume that the pore formation occurs at the lytic tension, τ_{lysis}, of the vesicle—*i.e.*, $\Sigma = \tau_{\text{lysis}}$—and can be determined through micropipette aspiration (see Table 1).[3] In contrast, the edge tension, Γ, is a semi-empirical parameter that is dependent on pore geometry. While the nature of a pore edge is generally unknown, there are two limiting cases: "hydrophobic" or "hydrophilic" pores (Fig. 3A). In the "hydrophobic" case, the pore is oriented such that the molecules lining the pore retain their original orientation normal to the membrane surface, thereby exposing their hydrophobic blocks. The line tension, Γ, is therefore the interfacial tension times the hydrophobic thickness, $\Gamma = \Sigma d$.[21] On the other hand, "hydrophilic" pores have molecules that curve over the length of the pore edge, resembling the edge of cylindrical micelles (Fig. 3A, *bottom left*). In this case $\Gamma \sim 2\,\kappa_b/d$, where κ_b is the bending of the membrane—which scales as d^2,[15] and is known for some of our polymers.[22] In either case, $\Gamma \sim d$. Additionally, for the PEG to have a steric effect it must sufficiently extend either laterally or along its length. De Gennes estimates the lateral (rms) spread in flat brushes to be $\Delta x \approx (L_0 s^{-1/2})^{1/2}$,[23] where $L_0$is the unperturbed brush length and σ is the chain grafting density. For our largest polymers ($d \geqslant 15$ nm), $\Delta x \approx 5$ nm, suggesting that "hydrophobic" pores are still able to meet the minimal criteria for steric interactions. The more likely situation is somewhere in between the above limits, where the pore edge is somewhat curved, and we can nonetheless assume $\Gamma \sim d$. It has been argued that the membrane energy for such a partially compressed membrane does in fact scale linearly with d.[24]

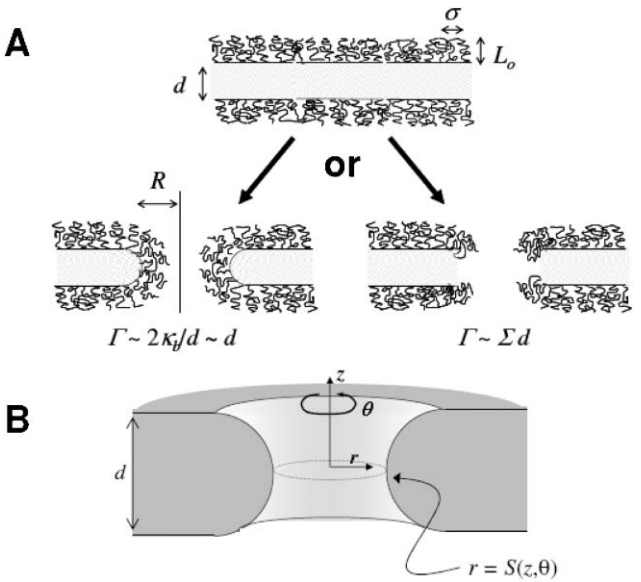

Fig. 3 (**A**) Cartoon of pore interior schematically depicting the PEG surface brush. The hydrophobic thickness d and brush length L vary for each system studied. Below are possible schematics for hydrophilic (*left*) and hydrophobic (*right*) pore schematics. In either case, the line tension does not change the scaling in d, and so for the purposes of this calculation, the two are indistinct. (**B**) For alternative geometries, if we restrict our calculations to surfaces of the form $r = S(z,\theta) = R{\cdot}f(\xi)$, we can decouple the integrand into z-dependent and z-independent parts, which allows for greatly simplified calculations.

In determining brush energy, the crucial parameters are the brush length, L, and the polymer grafting density, σ. Balancing elastic and excluded volume terms[25,26] gives the free energy of a single brush chain as:

$$\mu(\sigma,L) \approx N^{9/4}a^{15/4}\sigma^{5/4}L^{-5/4} + N^{-3/4}a^{-5/4}\sigma^{1/4}L^{7/4} \quad (3)$$

A minimization of eqn (3) in the absence of any external limitations in brush height immediately gives $L_0 \sim Na^{5/3}\sigma^{1/3}$, the well-known relation for polymer brush thickness and density. Here N is the number of segments and a the segment length (0.367 nm for EO). For a polymer membrane with fixed

brush density $\sigma = \sigma_0$ everywhere, the energy of the chain is $\mu(\sigma_0,L_0) = \mu_0(L_0) = L_0\sigma_0^{1/2}$, and from eqn (3), the free energy of a compressed brush initially at brush thickness L_0:

$$\mu_0(L) = \mu(\sigma_0,L) \approx L\sigma_0^{1/2}[(L_0/L)^{9/4} + (L/L_0)^{3/4}] \quad (4)$$

As a first approximation to our problem, we simplify the surface geometry first treated by de Gennes, namely, that of two opposing plates with grafted polymer chains of unperturbed length L_0 being brought into contact at a separation R.[27,28] The free energy contribution of the brush to this compression is $\Delta G = 2\sigma_0(\mu_0(L) - \mu_0(L_0))$ where the prefactor of 2 accounts for the two plates involved:

$$\Delta G_{\text{brush}} \sim 2\sigma\{R\sigma_0^{1/2}[(L_0/R)^{9/4} + (R/L_0)^{3/4}] - L_0\sigma_0^{1/2}\} \quad (5)$$

Note that eqn (5) represents the *change* in energy, per unit area: the reference state, which here is simply the plates at infinite separation ($G_0 \sim 2L_0\sigma_0^{3/2}$), has been subtracted. At separation distances $0 < R < L_0$, eqn (5) is valid; for $R \geqslant L_0$, the plates have no contact with each other and therefore $\Delta G_{\text{brush}} = 0$.

One key difference between our bilayer membranes and chemically grafted brushes described by eqn (5) is that in our polymersome systems the grafting density, σ, is not predetermined. It is naturally selected by (equilibrium or kinetic) conditions of the self-assembly process.[29–31] The PEG's average distance between chains in these systems (*i.e.* an "effective grafting density" for the fluid membrane) is a balance of excluded volume effects, in which the chain pressure tends to decrease σ, and the interfacial tension of the membrane, in which the energetic penalties of increasing the surface area tend to laterally compress the brush.[32] For our polymers, scaling arguments have been determined for this separation distance, in both intact (zero curvature) membranes ($\sigma \sim N^{-0.3}$)[3] and cylindrical (one axis of curvature) micelles ($\sigma \sim N^{-0.2}$).[33] Within the pore, however, the two axes of curvature, in opposite directions (toroidal geometry), suggest σ will probably have an intermediate scaling, and the density of chains is presumably a function of both position and pore size. For our initial calculations, we will crudely assume that $\sigma = \sigma_0$ is constant everywhere and at the value experimentally observed for the flat brush (Table 1).

While the assumption of a flat surface is an oversimplification, we will address more complex pictures in turn and show that there is little effect from curvature. As a next step, we modify the one-dimensional picture of two interacting flat plates by examining various pore surfaces that are axially symmetric about the pore center. This in essence becomes a Derjaguin type approximation to account for pore curvature. Most generally, we integrate the interaction energy over the surface to obtain:

$$\Delta G_{\text{brush}} = \int_{SA}\delta\mu(\mathbf{r};R,\sigma)\sigma(\mathbf{r};R)\mathrm{d}A \quad (6)$$

with $\delta\mu = \mu - \mu_0(L_0)$, and σ the two-dimensional density of polymer chains, which presumably would also vary with the pore size R. Geometrically, we begin with the simplest case of a cylindrical pore, from which more complex geometries give only a change in the coefficients in the free energy. For $R < L_0$, eqn (6) yields

$$\Delta G_{\text{brush}} \cong 8\pi d\sigma_0^{-3/2}(0.2L_0^{9/4}R^{-1/4} + 0.14\,L_0^{-3/4}R^{11/4} - 0.4\,L_0R) \quad (7)$$

and again, $\Delta G_{\text{brush}} = 0$ for $R > L_0$. The first term in eqn (7) is essentially an osmotic pressure term. As R decreases, the lateral pressure increases and the chain–chain repulsion resists closure. As the pore grows, the pore wall no longer compresses the molecules, and the chains fill the created void at the cost of the elastic energy, the second term of eqn (7). The final term in the eqn represents the baseline energy of the molecules in the pore, the population of which varies linearly with pore size.

For more complex pore geometries, we can, from eqn (6), derive relations similar to eqn (7) except here we shall consider alternative geometries. In cylindrical coordinates, the Jacobian, $\mathrm{d}A = r\mathrm{d}z\mathrm{d}\theta$, and we define a surface, $r = S(z,\theta)$ around the z-axis. Assuming as before that $\sigma(\mathbf{r}) \sim \sigma_o$ everywhere, we can rewrite eqn (6) as

$$\Delta G_{\text{brush}} = \sigma_0 \int_0^{2\pi}\int_{-d/2}^{d/2}(\mu_0(L(z,\theta)) - \mu_0(L_0))S(z,\theta)\mathrm{d}z\mathrm{d}\theta \quad (8)$$

where

$$\begin{aligned} &L(z,\theta) = S(z,\theta) \text{ if } S(z,\theta) < L_0 \\ &L(z,\theta) = L_0 \text{ elsewhere} \end{aligned} \quad (9)$$

and L_0 is the unperturbed length of the brush (Fig. 3B). That is, a chain is compressed to the size of the pore radius only if the natural length of the chain, L_0, is larger than the distance to the center of the pore.

We shall now make two assumptions. First, we restrict our calculations to those surfaces of the form

$$S(z,\theta) = Rf(z/d) = Rf(\xi),\ -\tfrac{1}{2} < \xi < \tfrac{1}{2} \quad (10)$$

which leaves out important surfaces of zero Gaussian curvature, but allows for great simplifications in the calculations, as we shall see. Second, we shall assume that there is no value for R (the nominal radius) where there is intermediate contact across the membrane thickness; that is, we shall consider cases where either $L(z,\theta) = S(z,\theta)$ for all or no z (in the latter case $\Delta G_{\text{brush}} = 0$). Again, this leaves out critical parts of the calculation, but it is intuitive that the real curves would be some intermediate value, or smoothing, between the two cases for a very small range in R.

With these assumptions, eqn (8) becomes

$$\Delta G_{\text{brush}} = 2\pi d\sigma_0\int_{-1/2}^{1/2}[\mu_0(Rf(\xi)) - \mu_0(L_0)]Rf(\xi)\mathrm{d}\xi \quad (11)$$

where $R < L_0$. Since we have defined the surface S to have separable variables in both R and z, when combined with eqn (4), we are now able to separate the z-containing terms and remove the others from the integral:

$$\Delta G_{\text{brush}} \sim 8\pi d\sigma_0^{3/2}(0.2\alpha L_0^{9/4}R^{-1/4} + 0.14\,\beta L_0^{-3/4}R^{11/4} - 0.4\,L_0R) \quad (12)$$

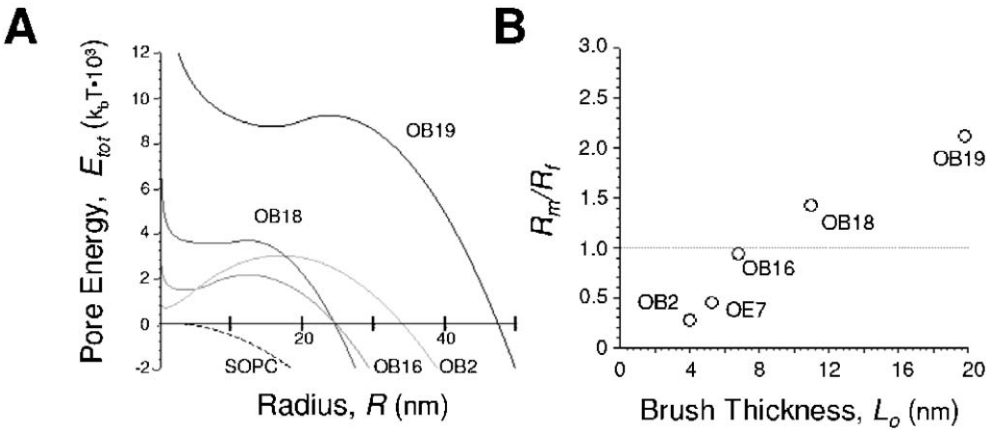

Fig. 4 Prediction of stable pores in polymersome membranes. (**A**) Energy landscapes for "hairy" pores, E_{tot}, as a function of membrane thickness d (eqn (7)). The behavior at $R > L_0$ is that of traditional pore theory (eqn (1)). (**B**) Graph of dimensionless R_m/R_f of stable points for vesicles from polymers outlined in Table 1. As mentioned in the text, the value of R for which eqn (7) has a relative minimum (R_m) is considered to be the predicted size of a stable pore (R_{stable}) if and only if it is greater than the Flory radius (*i.e.*, $R_{stable} = R_m$ if $R_m/R_f > 1$). Otherwise, no stable pore is predicted to exist. Long lived, multiple, pores are only observed for $d = 15$ nm (OB18) and $d = 21$ nm (OB19) membranes (see Table 2).

where

$$\alpha = \int_{-1/2}^{1/2} (f(\xi))^{-1/4} d\xi, \text{ and } \beta = \int_{-1/2}^{1/2} (f(\xi))^{11/4} d\xi \qquad (13)$$

For the paraboloid surface $S(\xi) = R(1 + \xi)^2$, $\alpha = 0.910$ and $\beta = 1.154$, and for the catenoid surface $S(\xi) = R\coth(\xi)$, $\alpha = 0.953$ and $\beta = 1.073$, and in general of order one, and so do not significantly affect the results presented here.

3. Discussion

Combining eqn (1) and (7), we arrive at a new relation for the energy of a pore that includes the effects of sterically stabilizing polymer chains. Plotting the energy landscape for pores in selected polymersomes shows local minima occurring at values below the unstable point R^* predicted by eqn (1) alone (Fig. 4A). These minima, denoted as R_m, are intriguing but are not strictly stability points, as we discuss below.

The energy balance, as given in eqn (7), is by no means complete; however, the inclusion of more complex parameters would not affect the results qualitatively. Including a dynamic surface tension, which scales as $\Sigma \sim R^2$,[8,34] for example, would not change the essential results here, since the steric effects will persist only at small length scales, even if the surface tension is dissipated. In short, the assumptions used in deriving eqn (7) are crude yet sufficient, as written, in explaining the nature of the observed stable or metastable pores.

Similarly, related axisymmetric geometries (*e.g.*, a catenoid or a paraboloid) are tractable and give the same form of eqn (7) with numerical prefactors of order unity.

The domain of eqn (7), however, is limited. We anticipate that the result is only valid for the regime where $R > R_f$, where R_f is the Flory radius ($\sim N^{0.6}a$). For pores smaller than this critical size, the entropic energy of the chain changes sign; further reduction in the size of the pore would result in prohibitively compressed chains. This is especially true in the "hydrophilic" pore; in the "hydrophobic" case, when the pore size is less than the Flory radius, the hole simply ceases to exist. Thus, if the mathematical minimum of eqn (7), R_m, is greater than R_f, then we define $R_{stable} = R_m$, the predicted stable size of the membrane pore.

For $R < R_f$ pores, the energy, ΔG_{brush}, may be strictly a result of the entropic cost to physically displace the chains out of the pore; as only the chains near the edge of the pore are affected. The number of molecules (and consequently the total energy) scales as the area of the pore, R^2, which can be treated simply as a rescaling of the surface tension in eqn (1) (implying pore resealing). The line tension may also be affected by the crowding of molecules around the pore, as discussed by Fournier and Joos.[21] Generally, molecular crowding is only a local effect in our systems due to the length of the chains, but can become a factor for smaller pores.

The resulting overall energy landscapes show minima, R_m, increasing with d as indicated in Fig. 4B, and summarized in Table 2. In agreement with experiments, only OB18 ($d = 15$ nm) and OB19 ($d = 21$ nm) exhibit stable pores of sizes greater than the Flory radius, at $R_{stable} = 7.2$ nm and $R_{stable} = 15.6$ nm, respectively. In the case of OB18, we have estimated the pore diameter to be ~ 5 nm (by visualizing the release of different-sized encapsulated molecules),[6] in good agreement with our theoretical results. The smaller diblocks have minima below R_f, outside the valid domain of eqn (7). Indeed, these diblocks produce vesicles without any apparently stable pores.

Table 2 Values at which eqn (5) is minimized for the polymersomes outlined in Table 1, R_m, the lower and upper boundaries on R (R_f and R^*, respectively) and the experimentally-determined pore size. Only OB18 and OB19 form vesicles which exhibit stable pores upon electroformation. Note that $R_{stable} = R_m$ only if $R_f < R_m < R^*$. The Flory radius is $aN^{0.6}$, and R^* is the maximization of eqn (1)

Vesicle name	R_f/nm	R_m/nm	R^*/nm	"Stable" pore size
SOPC	—	—	19.6	—
OB_2	3.3	1.5	11.5	—
OE7	2.6	0.72	17.0	—
OB16	3.8	3.6	12.3	—
OB18	5.1	7.25	12.2	~ 5 nm[7]
OB19	7.4	15.7	23.7	>6 nm[7]

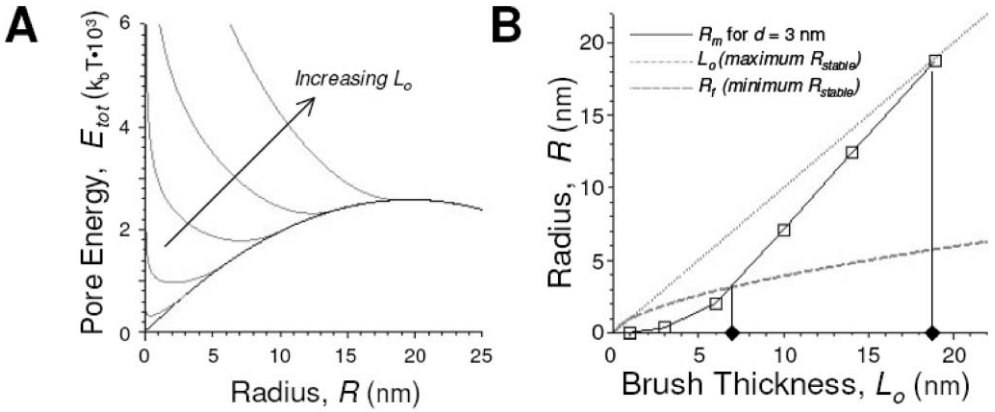

Fig. 5 Prediction of stable pore size in theoretical systems. (**A**) Energy landscapes for a "hairy" pore, E_{tot}, for a theoretical membrane of d = 3 nm (SOPC-like) with variations in brush thickness. As the brush gets thicker, the minimum shifts to the right of the graph, and, above a critical value, the minimum ceases to exist. The minimum can never be greater than the value of the relative maximum, R^*. (**B**) With the upper boundary, R^*, and the lower boundary R_f, there is only a small range of values of L_0 that can stabilize a pore. Using the same system from (**A**) (*i.e.* a typical red cell), we arrive at values for the lower and upper boundary of L_0 that can stabilize the membrane pore, 7–18 nm, precisely the reported size of an erythrocyte glycocalyx.[37]

From eqn (5) we can determine the dependence of R_m (and therefore R_{stable}) on diblock properties. Trends from virtual polymers with fixed core size but varying PEG brush thickness (Fig. 5A) suggest that $R_m \sim \alpha L_0^2 d$, where $\alpha \approx 15$ Å^{-2} over typical values of L_0 and d. This relationship implies that thicker brushes will yield larger holes, which is observed in the apparent pore sizes of OB18 and OB19. Mathematically, it is apparent that $R_m < R^*$, the unstable point of eqn (1) and the point at which the surface tension dominates both the line energy and the brush energy. With both an upper (R^*) and a lower (R_f) boundary on R_{stable}, and a one-to-one correspondence between R_{stable} and L_0($L_0 \sim (R_{stable}/d)^{1/2}$), the brush thickness that is capable of stabilizing a pore in a membrane of thickness d and PEG spacing D_0, is bounded:

$$[(N^{0.6}a)/(\alpha d)]^{1/2} \leqslant L_o \leqslant [(\Gamma/\Sigma)/(\alpha d)]^{1/2} \qquad (14)$$

For brushes smaller than this value, the minimum pore size as calculated by eqn (7) is smaller than the size of an individual polymer chain. For larger brushes, the sugar chains do not allow the pore to reach a small enough size where line tension can balance the surface tension. The narrow range of membranes capable of producing stable pores in the manner of polymersome poration suggests why in general they are rarely observed.

One system in which stable pores are reported is in the erythrocyte membrane. Osmotic tension of erythrocytes, depending on conditions, can result in pores ranging from 2 to 10 nm that can last for several days.[35] Erythrocytes possess a surface brushy layer (glycocalyx)[36] whose height is estimated to be 6–20 nm.[37] This is substantial when compared to the lipid bilayer thickness of 3–4 nm.[38] The existence of these thermodynamically stable pores—not found in liposomes of similar composition[14,39,40]—suggests that the brushy glycocalyx again plays a steric role in stabilization.

While glycolipids may preferentially partition into the pore (reducing Γ), the argument for the maximum and minimum size of the pore still holds, as eqn (8) can account for changes in the line tension. For a red blood cell membrane, eqn (8) predicts that stable pores are possible for a glycocalyx of 7–20 nm in thickness; a reduced line tension would reduce the maximum value. As mentioned before, this range is a result of 1) a thicker brush (in this case, glycolipid sugars) dominating the system at pore radii larger than the critical unstable point leading to rupture, and 2) a thinner glycocalyx not giving "enough" stabilization. For erythrocytes, this theoretical window indeed coincides with the observed glycocalyx thickness (Fig. 5B). This limited size range is especially intriguing, since glycocalyx thickening has been implicated in the senescence of erythrocytes,[41] which may therefore cause existing pores to expand beyond the critical size and induce membrane instability. Additionally, for a nominal glycocalyx thickness of 10 nm, the predicted stable pore size, $R_{stable} \approx$ 6 nm, is very consistent with experimental observations.[35] Liposomes (also with $d \approx 3$ nm) lack any membrane sugars or proteins, and therefore do not form stable pores in general.[14] The closest analogy to purely lipid systems has been reported by Brochard-Wyart and coworkers,[42] in which the addition of "edge-actant" agents preferentially partition at the pore edge and reduce the line tension.

Other approaches to related problems include the framework of Daoud and Cotton for star polymers, in which the brush free energy is determined from scaling arguments based on the geometry of the packed brush.[43] The radial density profile within the pore is similar to that of a star polymer (without the constraint of a central junction). While others[44] have shown that the direction of the curvature may be important (*i.e.*, inward *vs.* outward) for the overall chain energy, the opposing curvatures seen here lead us to anticipate qualitatively similar results with the above calculations. It is, however, important to note that since the pore size is of the same order as the thickness, *i.e.* $R_{stable} \sim d$, the two curvatures of the "hemi-torus" that make up the pore are therefore also of the same, but opposite, order. Therefore any attempt at using models in which the two curvatures are decoupled must be made with great trepidation. Self-consistent field theory

approaches to pores in polymer bilayers by Netz and Schick have been predicted by means of a phase transition from lamellar to catenoid lamellar, with the pores in a hexagonal array.[45] However, this is difficult to confirm experimentally. We re-emphasize that while our model is by no means exhaustive, it adequately describes the experimental phenomena.[6]

However, a thorough discussion of these pores is not complete without a careful consideration of kinetically trapped pores. Viscous effects of the large polymer molecules—a result of chain entanglement—might delay the resealing of the pore. Similar delayed responsiveness has been seen with micropipette aspiration of vesicles of OB18 and OB19,[3] with relaxation times of the order of minutes. However, during aspiration, the surface area that is disrupted is much larger than that during pore formation: the number of molecules required to reseal a pore of 5–10 nm in radius is comparatively tiny. While the diffusion constant of OB19 has not yet been determined, the diffusivity of an OB18 molecule is 0.0024 $\mu m^2\ sec^{-1}$, which is several orders of magnitude slower than an SOPC molecule (3.8 $\mu m^2\ sec^{-1}$) or even an OE7 chain (0.12 $\mu m^2\ sec^{-1}$), but still sufficient to explore an area of several pores within seconds.[22] Therefore while the entrapment of polymer chains that might keep the pore open remains a possibility, the apparent long life of the pores suggests that the pores are in true thermodynamic equilibrium.

One obvious application of these systems is in drug delivery. Practical delivery vehicles must address the often-opposing requirements of container stability and controlled release. With highly structured polymer-based vesicles, one has flexibility in the choice of parameters by virtue of the synthetic approach. Stability can be controlled by the interfacial chemistry[3] independently from the release kinetics, which would be tunable through pore size. Further control could be accomplished through chemical means such as covalent crosslinking,[2] or degradable polymers,[10] or the use of worm-like micelles or DNA entropically constrained within the vesicle.[11,33,40,46]

Lastly, we return briefly to the relevance of these calculations to the nuclear pore complex or NPC (Fig. 1). The dense brush of flexible chains of the nucleoproteins that are postulated to regulate transport into and out of the NPC[1] are shown here to exert an osmotic force on the pore that counteracts the association energy of the many proteins that assemble into the making the NPC. While the NPC is one of the largest and most complex protein assemblies in the eukaryotic cell, rivaling the ribosome,[38] the cohesive stability of the NPC has yet to be understood. Perhaps mutants in some of the proteins destabilize the NPC against such stresses and lead to disease, or perhaps cellular invaders such as viruses have a similar effect. Deeper insights could also—as speculated at the outset—lead to regulated synthetic pores as functional as the NPC.

4. Conclusion

The long-lasting pores seen in membranes with thick brushes may be a result of steric stabilization of the hole by the PEG chains. Using a simple model that includes the energy of the PEG brush, we show that such stabilization is possible, and the predicted size of the pores is in good agreement with previous experiments. Furthermore, for stabilization to occur, the brush can only be within a narrow range of thicknesses, also in agreement with experimental observations. Intriguingly, this model can also successfully predict glycocalyx thickness and pore sizes observed in erythrocyte membranes. Although the concept and application of polymers to sterically stabilize systems is well established, few examples naturally exhibit such mechanisms. Polymeric self-assemblies are therefore ideally suited for responsive materials that have inherent capabilities to either disassemble or change microstructure depending on local conditions. Biology provides notable examples, such as the combination of unstructured and structured protein elements together in assemblies that include nuclear pores, porated cell membranes, and also intermediate filaments.[47] Future directions in materials science will clearly exploit these, and other, mechanisms.[48]

Acknowledgements

Funding was provided by NSF-MRSEC and The American Heart Association. The authors thank the Bates group at the University of Minnesota for copolymer synthesis as well as P. Pincus and J. N. Israelachvili for helpful comments and suggestions.

References

1 R. Y. H. Lim, N.-P. Huang, J. Köser, J. Deng, K. H. A. Lau, K. Schwarz-Herion, B. Fahrenkrog and U. Aebi, *Proc. Natl. Acad. Sci. U. S. A.*, 2006, **103**, 9512.
2 D. E. Discher and A. Eisenberg, *Science*, 2002, **297**, 967.
3 H. Bermudez, A. K. Brannan, D. A. Hammer and F. S. Bates, *Macromolecules*, 2002, **35**, 8203.
4 V. Ortiz, S. O. Nielsen, D. E. Discher, M. L. Klein, R. Lipowsky and J. Shillcock, *J. Phys. Chem. B*, 2005, **109**, 17708.
5 E. Neumann, A. E. Sowers and C. A. Jordan, *Electroporation and Electrofusion in Cell Biology*, Plenum Press, New York, 1989.
6 H. Bermúdez, H. Aranda-Espinoza, D. A. Hammer and D. E. Discher, *Europhys. Lett.*, 2003, **64**, 550.
7 H. Aranda-Espinoza, H. Bermudez, F. S. Bates and D. E. Discher, *Phys. Rev. Lett.*, 2001, **87**, 208301.
8 O. Sandre, L. Moreaux and F. Brochard-Wyart, *Proc. Natl. Acad. Sci. U. S. A.*, 1999, **96**, 10591.
9 E. Karatekin, O. Sandre, H. Guitouni, N. Borghi, P.-H. Puech and F. Brochard-Wyart, *Biophys. J.*, 2003, **84**, 1734.
10 F. Ahmed and D. E. Discher, *J. Controlled Release*, 2004, **96**, 37.
11 E. Neumann, S. Kakorin and K. Tœnsing, *Bioelectrochem. Bioenerg.*, 1999, **48**, 3.
12 M. Bates, M. Burns and A. Meller, *Biophys. J.*, 2003, **84**, 2366.
13 O. Flomenbom and J. Klafter, *Phys. Rev. E: Stat., Nonlinear, Soft Matter Phys.*, 2003, **68**, 041910.
14 D. V. Zhelev and D. Needham, *Biochim. Biophys. Acta*, 1993, **1147**, 89.
15 T. A. Witten and P. A. Pincus, *Macromolecules*, 1986, **19**, 2509.
16 A. G. Yodh, K.-H. Lin, J. C. Crocker, A. D. Dinsmore, R. Verma and P. D. Kaplan, *Philos. Trans. R. Soc. London, Ser. A*, 2001, **359**, 921.
17 A. K. Dolan and S. F. Edwards, *Proc. R. Soc. London, Ser. A*, 1974, **337**, 509.
18 B. V. Deryagin, V. V. Karasec, A. M. Medvedev and S. K. Zherebko, *Colloid J.*, 1965, **27**, 298.
19 J. D. Litster, *Phys. Lett. A*, 1975, **53**, 193.
20 J. C. Weaver, *IEEE Trans. Dielect. Electr. Insul.*, 2003, **10**, 754.
21 L. Fournier and B. Joos, *Phys. Rev. E: Stat., Nonlinear, Soft Matter Phys.*, 2003, 67.
22 J. C. M. Lee, R. J. Law and D. E. Discher, *Langmuir*, 2001, **17**, 3592.

23 P. G. Degennes, *Macromolecules*, 1980, **13**, 1069.
24 V. Pata and N. Dan, *Biophys. J.*, 2003, **85**, 2111.
25 S. Alexander, *J. Phys. (Paris)*, 1977, **38**, 977.
26 P. L. Hansen, J. A. Cohen, R. Podgornik and V. A. Parsegian, *Biophys. J.*, 2003, **84**, 350.
27 P. G. Degennes, *C. R. Acad. Sci., Ser. II: Mec., Phys., Chim, Sci. Terre Univers*, 1985, **300**, 839.
28 P. G. Degennes, *Adv. Colloid Interface Sci.*, 1987, **27**, 189.
29 S. Belsito, R. Bartucci, G. Montesano, D. Marsh and L. Sportelli, *Biophys. J.*, 2000, **78**, 1420.
30 G. Montesano, R. Bartucci, S. Belsito, D. Marsh and L. Sportelli, *Biophys. J.*, 2001, **80**, 1372.
31 A. Halperin, M. Tirrell and T. P. Lodge, *Adv. Polym. Sci.*, 1992, **100**, 31.
32 K. Hristova and D. Needham, *J. Colloid Interface Sci.*, 1994, **168**, 302.
33 P. Dalhaimer, H. Bermudez and D. E. Discher, *J. Polym. Sci., Part B: Polym. Phys.*, 2004, **42**, 168.
34 H. Isambert, *Phys. Rev. Lett.*, 1998, **80**, 3404.
35 M. R. Lieber and T. L. Steck, *J. Biol. Chem.*, 1982, **257**, 11660.
36 P. L. McNeil and M. Terasaki, *Nat. Cell Biol.*, 2001, **3**, E124.
37 W. Linss, C. Pilgrim and H. Feuerstein, *Acta Histochem.*, 1991, **91**, 101.
38 B. Alberts, *Essential Cell Biology: An Introduction to the Molecular Biology of the Cell*, Garland Pub., New York, 1998.
39 N. M. Correa and Z. A. Schelly, *J. Phys. Chem. B*, 1998, **102**, 9319.
40 N. I. Hristova, I. Tsoneva and E. Neumann, *FEBS Lett.*, 1997, **415**, 81.
41 B. Neu, S. O. Sowemimo-Coker and H. J. Meiselman, *Biophys. J.*, 2003, **85**, 75.
42 P. H. Puech, N. Borghi, E. Karatekin and F. Brochard-Wyart, *Phys. Rev. Lett.*, 2003, **90**, 128304.
43 M. Daoud and J. P. Cotton, *J. Phys. (Paris)*, 1982, **43**, 531.
44 M. Manghi, M. Aubouy, C. Gay and C. Ligoure, *Eur. Phys. J. E*, 2001, **5**, 519.
45 R. R. Netz and M. Schick, *Phys. Rev. E: Stat. Phys., Plasmas, Fluids, Relat. Interdiscip. Top.*, 1996, **53**, 3875.
46 W. Sung and P. J. Park, *Phys. Rev. Lett.*, 1996, **77**, 783.
47 H. G. Brown and J. H. Hoh, *Biochemistry*, 1997, **36**, 15035.
48 M. Muthukumar, C. K. Ober and E. L. Thomas, *Science*, 1997, **277**, 1225.